Changing rapid weather variability increases influenza epidemic risk in a warming climate

IOP Publishing Journal Title
Journal **XX** (XXXX) XXXXXX https://doi.org/XXXX/XXXX

Changing Rapid Weather Variability Increases Influenza Epidemic Risk in a Warming Climate

Qi Liu[1,2,3‡], Zhe-Min Tan[1‡], Jie Sun[2], Yayi Hou[4], Congbin Fu[1,3*], Zhaohua Wu[2*]

[1] School of Atmospheric Sciences, Nanjing University, Nanjing 210023, P. R. China.
[2] Department of Earth, Ocean, and Atmospheric Science & Center for Ocean-Atmospheric Prediction Studies, Florida State University, Tallahassee FL 32306, USA.
[3] Institute for Climate and Global Change Research, Nanjing University, Nanjing 210023, P. R. China.
[4] The State Key Laboratory of Pharmaceutical Biotechnology, Division of Immunology, Medical School, Nanjing University, Nanjing 210023, P. R. China.

‡ These authors contributed equally to this work.
* Corresponding authors: Congbin Fu; Zhaohua Wu

E-mail: fcb@nju.edu.cn (Congbin Fu); zwu@fsu.edu (Zhaohua Wu)

Received xxxxxx
Accepted for publication xxxxxx
Published xxxxxx

Abstract

The continuing change of the Earth's climate is believed to affect the influenza viral activity and transmission in the coming decades. However, a consensus of the severity of the risk of influenza epidemic in a warming climate has not been reached. It was previously reported that the warmer winter can reduce influenza epidemic-caused mortality, but this relation cannot explain the deadly influenza epidemic in many countries over northern mid-latitudes in the winter of 2017-2018, one of the warmest winters in recent decades. Here we reveal that the widely spread 2017-2018 influenza epidemic can be attributed to the abnormally strong rapid weather variability. We demonstrate, from historical data, that the large rapid weather variability in autumn can precondition the deadly influenza epidemic in the subsequent months in highly populated northern mid-latitudes; and the influenza epidemic season of 2017-2018 was a typical case. We further show that climate model projections reach a consensus that the rapid weather variability in autumn will continue to strengthen in some regions of northern mid-latitudes in a warming climate, implying that the risk of influenza epidemic may increase 20% to 50% in some highly populated regions in later 21st century.

Keywords: Climate change; influenza epidemic; rapid weather variability; North Mid-latitude; predictable model

1. Introduction

The influenza epidemics tend to occur more frequently from October to May, peaking in January and February over the highly populated northern mid-latitudes (Baumgartner *et al* 2012, Viboud *et al* 2006). This boreal winter half of a year is often referred to as influenza season. The seasonality of influenza suggests a potential tie to the seasonality of weather and climate (Deyle *et al* 2016, Altizer *et al* 2006). However, a consensus of the severity of the risk of influenza epidemic in a warming climate has not been reached (Staddon *et al* 2014, Ballester *et al* 2016, Bennett *et al* 2014). Previous studies have suggested that low surface air temperature and humidity in winter constitute a favorable climatic environment for the survival and transmitting of the influenza virus (Walther and Ewald 2004, Polozov *et al* 2008, Shaman and Kohn 2009); and therefore, the continuing fast warming of the Earth's climate in winter can depreciate the favorable climatic environment for the survival and transmission of influenza virus and reduce future influenza epidemic risk (Ballester *et al* 2016). However, this relation cannot explain the deadly influenza epidemic in many countries over northern mid-latitudes in the winter of 2017-2018 (Cohen 2018, Garten *et al* 2018), one of the warmest winters in recent decades.

In general, the transmission of influenza virus and the spread of human influenza-like disease (ILI) depends on many factors. One of them is the surviral and reproductivity of influenza virus in different ambient conditions. Previous studies have shown that the reproductivity of influenza virus and survival length of the virus in a colder and less moist air is larger and thereby the transmission of influenza virus is more effective in winter seasons when both moisture level and temperature are low. This disease dynamics has been confirmed in the experiments with guinea pigs (Lowen *et al* 2007, 2014, Shaman and Kohn 2009) and the relation was even incorporated into models that fit the past data and make prediction of the strengh of incoming flu season (Shaman *et al* 2010, Yang *et al* 2015, Delziel *et al* 2018). It should be noted that becoming infected with the influenza virus depends also on the strength of the human immune system (Mirsaeidi 2016), as evidenced by the use of influenza vaccines. Seasonal fluctuations in human immunity could also play a role in the seasonality of influenza epidemics (Petrova and Russell 2018). In such a sense, understanding the variability and change of any climatic aspect that can affect human immune system will help more accurately estimate the relation between the continuing climate change and future influenza epidemic risk. It is also noted that the seasonality association is not only with ILI but also with other diseases (Wei *et al* 2019).

2. Materials and Methods

2.1 Meteorological data

Daily maximum surface air temperatures of the Europe and the continental United States for the period January 1, 1997 to February 28, 2018 are derived from the Global Historical Climatology Network (ftp://ftp.ncdc.noaa.gov/pub/data/ghcn/daily/), covering a total number of 7729 days. The data are all the meteorological station-observed daily maximum temperature. Many individual stations contain non-observed days. In this study, only the daily temperature time series of individual stations that satisfy the following conditions are analyzed: (1) station-observed temperature time series has no more than 80 missing days for any individual winter half year (from August 1 to February 28); and (2) fewer than 750 days of missing data over the studying period (1997-2018). There are 559 stations satisfying these two conditions in United States and 547 in Europe. The available temporal domain of Italy is from 1999 to 2018. The spatial interpolation using Matlab function *griddata* is then applied to fill in missing data for any individual days for all meteorological stations. The homogenized data is then averaged to obtain state-wise (United States) or country-wise (Europe) averaged daily maximum temperature. The Global Historical Climatology Network contains relatively fewer numbers of stations over China. Therefore, the station-observed daily maximum temperature over China is from the quality controlled (Li *et al* 2004) observations assembled by the National Meteorological Information Center of the China Meteorological Administration (http://data.cma.cn/). There are 654 stations over China that satisfy the above two conditions.

Daily near-surface mean absolute humidity is from reanalysis provided by the National Centers for Environmental Prediction/National Center for Atmospheric Research (NCEP/NCAR reanalysis) (Kalnay *et al* 1996). This dataset is a spatially gridded one having a fixed zonal resolution of 1.875 degree of longitude and a varying Gaussian-shaped meridional resolution with its average close to 1.875 degree of latitude. The data covers the whole global domain starting from January 1, 1948. In this study, we analyze data covering the same temporal span, from January 1, 1997 to February 28, 2018, to obtain state-wise (United States) or country-wise (Europe and China) averaged absolute humidity field. The reanalysis can be downloaded from: https://www.esrl.noaa.gov/psd/data/gridded/data.ncep.reanalysis.html.

The simulated and projected daily surface maximum temperatures are from the CMIP5 (Schneider *et al* 2015) for the periods Jan. 1950—Dec. 2005 and Jan. 2006—Dec. 2100, respectively. The projected future climate data selected are from two future emission scenarios: The RCP4.5 and RCP8.5. Seven widely acclaimed earth system models from different countries are selected, with their names, institutes, and horizontal resolution listed in Supplementary Table S1. The simulated and projected data can be downloaded from: https://esgf-node.llnl.gov/projects/cmip5/.

2.2 Influenza-like illness and influenza morbidity (ILI/IM) data

Due to the different settings in the influenza datasets (Supplementary Table S2), the analyzed data from the United States of America (USA) is the influenza-like illness (ILI) defined as the percentage of patients with influenza-like illness among all patients. For European countries and the mainland China, the analyzed datasets contain weekly percentage of confirmed influenza patients among all tested patient samples, which is referred as influenza morbidity (IM) in this study. Due to the varying spatiotemporal resolutions of different datasets, interpolation or summation methods are used to obtain the same spatiotemporal resolutions if necessary.

Weekly IM data over Europe and China are obtained from the Influenza Laboratory Surveillance Information of the World Health Organization. Weekly IM data of 34 countries are analyzed in this study, with source laboratories and available temporal domains listed in Supplementary Table S2. The data can be downloaded from: http://apps.who.int/flumart/Default?ReportNo=14.

The ILI data are from the U.S. Center for Disease Control and Prevention. The dataset has weekly temporal resolution and includes three different subsets: (1) the state-wise reported percentage of ILI patients covering period from the 40^{th} week of 2010 to present; (2) the standard federal region-wise covering period from the 40^{th} week of 1997 to present; and (3) the whole United States averaged covering the period from the 40^{th} week of 1997 to present. The data can be downloaded from: https://gis.cdc.gov/grasp/fluview/fluportaldashboard.html. The reason for using ILI data rather than IM data over the United States is due to the inconsistency in IM data. According to the U.S. Center for Disease Control and Prevention, the methods for collecting IM data changed after 2015-2016 while these for collecting ILI data remained the same for 1997 to 2018.

2.3 Definition of rapid weather variability

It has been proposed that sudden large change in temperature can impair human immune system and trigger immune evasion (Loh *et al* 2013, Togias *et al* 1985, Eurowinter Group 1997, Graudenz *et al* 2006, Guo *et al* 2011, Guo *et al* 2016). The possible mechanism is that the human thermoregulation of immune defense is less adjustable to the sudden large change in temperature (Guo *et al* 2011, Guo *et al* 2016) and less resistant to various diseases (Eurowinter Group 1997, Graudenz *et al* 2006). Recently, studies showed that the sudden large change in temperature tends to cause high respiratory mortality (Eurowinter Group 1997, Graudenz *et al* 2006, Guo *et al* 2011, Guo *et al* 2016, Zhan *et al* 2017) and to impact influenza seasonality (Li *et al* 2018). It is, in fact, based on this pathological mechanism that we suspect frequent fluctuating weather, as an additional factor, may play a significant role in influenza epidemics.

To quantify the sudden large change in temperature, here we introduce a climatic quantity called rapid weather variability (RWV) for any given temporal location: the total number of consecutive-day with surface air temperature differences (Wu *et al* 2017) larger than 3 K over a three-week period ending at that temporal location (see Supplementary Table S1). The procedure of quantifying RWV is shown in Supplementary Fig. S1; the number of absolute differences of consecutive-day surface air temperature (Fig. S1b) is first calculated from the raw daily surface air temperature time series (Fig. S1a), and the number of days with the differences larger than 3 K over a three-week sliding window is obtained (Fig. S1c). The selection of a temporal window length of three weeks allows us to retain sufficient variability of RWV and reduce the effect of randomness. It is important to note that the threshold of 3 K is not an arbitrary selection; rather, it is based on the sensitivity of human immune system to temperature variability (Guo *et al* 2011). Both positive and negative change in temperature of more than 3 K would remarkably increase the respiratory mortality (Guo *et al* 2011). It is noted that the key results presented late in this paper are not sensitive to the selection of window size for defining RWV as long as it is between two weeks to four weeks (see Supplementary Text and Supplementary Figs. S2-S3).

2.4 The lagged correlations between weather variables and ILI/IM

In this study, we explore the impact of rapid weather variability on ILI/IM. Since the former cannot be changed by the latter, we anticipate an either simultaneous or delayed response of ILI/IM to rapid weather variability. To characterize this relation, lagged correlations of various delays are calculated for weekly anomalous weather variable $V_{i,j}$ and the weekly anomalous value $N_{i,j}$ of ILI/IM of the same region, where subscript i and j represent the ordered year and ordered week of a year, respectively. The lagged correlation between $V_{i,j}$ and $N_{i,j}$ is defined as

$$r_j(\tau) = \frac{\sum_{i=i_s}^{i_e} V_{i,j} N_{i,j+\tau}}{\sqrt{\sum_{i=i_s}^{i_e} V_{i,j}\, V_{i,j}}\sqrt{\sum_{i=i_s}^{i_e} N_{i,j+\tau}\, N_{i,j+\tau}}}$$

where i_s is the starting influenza season, and i_e is the ending influenza season. In this study, i_s corresponds to 1997-1998 influenza season and i_e 2017-2018 influenza season but with 2009-2010 influenza season excluded since the ILI/IM in that season was dominated by swine influenza that has an abnormal spreading dynamics (Munster *et al* 2009, Vijaykrishna *et al* 2011, Smith *et al* 2009). In addition, Monte Carlo Test was used to examine the statistical significance of lagged temporal correlation. The statistical significances of different countries for the correlation coefficients of ±0.4, ±0.45, ±0.5, and ±0.55 are listed in Supplementary Table S3.

3. Results

3.1 Rapid weather variability preconditions influenza epidemic

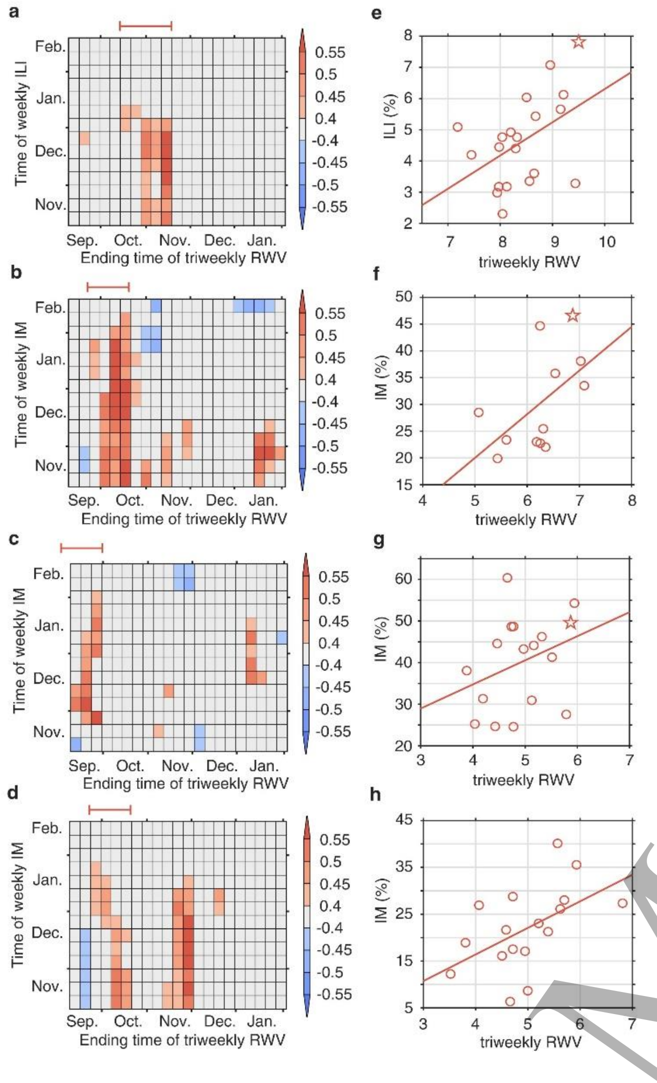

Figure 1. Long-term ILI/IM changes with respect to RWV. a, Weekly lagged correlation between triweekly RWV anomaly and ILI/IM anomaly for period 1997-2018 over the whole USA. b-d, the same as a but for the mainland China (2005-2018), Italy (2000-2018), and France (1997-2015), respectively. e, the scattered plot of the pairs of peak ILI/IM and the averaged triweekly RWV over the temporal span marked by red interval immediately above each left panels, for the USA over the temporal span of 1997-2018, with the stars correspond to 2017-2018 influenza season. f-h, the same as e, but for mainland China (2005-2018), Italy (2000-2018), and France (1997-2015), respectively.

Figure 1 presents various relations between autumn RWV and ILI/IM. For the four northern mid-latitude countries/regions, i.e., the United States, the mainland China, Italy, and France, which have relatively longer ILI/IM data, a common feature emerged is that the autumn RWV appears to have long-lasting effect on the influenza epidemic strength in the subsequent months (coherent reddish blocks in the correlation maps displayed in left column panels of Figure 1, statistical significances are shown in Supplementary Table S3), implying the RWV has preconditioned the occurrence of influenza epidemic, although the influenza peaking time were different for all these regions. The case in Fig. 1b in which January RWV is correlated with influenza mortality in the previous November was largely caused by a few individual Flu seasons, such as 2010-2011 winter, 2013-2014 winter, and 2015-2016 winter (Supplementary Fig. S8b). With small sample, such spurious relation can exist although unreal. Another feature common to all four regions is that the peak strength of ILI/IM, P, increases with the strength of RWV in autumn. The normalized change rates, $\left(P-\bar{P}\right)/\bar{P}$, corresponding to RWV value changed by 1 are 23%, 27%, 14%, and 26% for the United States, the mainland China, Italy, and France, respectively (Supplementary Fig. S13). These values indicate that the ILI/IM is highly impacted by RWV, at least from statistical perspective. It is also noted that the statistical relation between later autumn RWV and the following winter ILI is most robust in populations of age less than 5 and greater than 65 for the United States (see Supplementary Text and Supplementary Fig. S4).

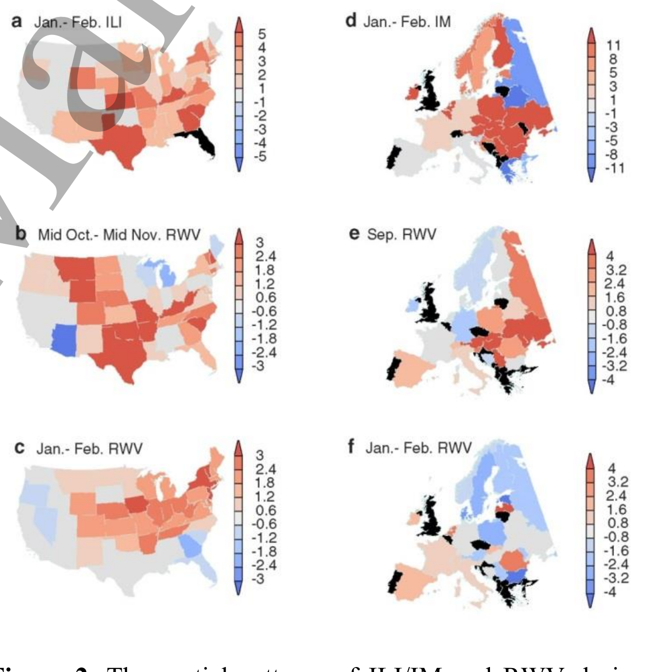

Figure 2. The spatial patterns of ILI/IM and RWV during 2017-2018 influenza season. a, U.S. ILI/IM anomaly (%) averaged over January-February 2018; b-c, Monthly averaged RWV anomaly (days) over U.S. from October 15-November 15, 2017 and January-February 2018, respectively; d, the same as a but for Europe. e-f, Monthly averaged RWV anomaly (days) over Europe from September 2017 and January-February 2018, respectively; Black represents missing records.

To further confirm the lasting effect of autumn RWV on later winter ILI/IM peaking strength, Fig. 2 presents the spatial patterns of RWV and ILI/IM of 2017-2018 influenza season for the United State and a large portion of the Europe. The influenza epidemic season of 2017-2018 was one of the severest influenza seasons in the United States and the Europe (Cohen 2018, Garten *et al* 2018), causing up to 4064 mortalities a week in the United States only. The spatial patterns of RWV in mid-October to mid-November of 2017 for the United States and in September of 2017 for the Europe share similar spatial structures of their corresponding peak ILI/IM in January and February of 2018, with spatial correlations between RWV in autumn and ILI/IM of 0.32 for the United States and 0.33 for the Europe, both exceeding a 95 percent confidence level against a null hypotheses of random spatial distribution. However, the simultaneous spatial correlations between RWV and peak ILI/IM are much smaller, having values of -0.06 in U.S. and -0.23 in Europe, and not statistically significant.

Results from the above analysis suggest a mechanism of ILI/IM temporal evolution: in later autumn, the intensified RWV contributes to the increase of influenza patients. When the mass of patients reaches a critical level in a densely populated region, the direct contacts between influenza patients and healthy persons increase and the rate of persons being infected with the influenza virus reaches a level greater than the rate of influenza recovery, leading to a fast increase in influenza patients and a severe influenza season. The 2017-2018 influenza season of the US appears to confirm the hidden operation of such a mechanism although it may not be the most dominant one. Since an influenza epidemics' peak season is mostly in the second half of winter and RWV in autumn contributes significantly to building critical patient levels in densely populated regions, the strength of RWV during autumn may serve as a valuable predictor of the severity of consequent influenza season, thus facilitating earlier preparation and prevention.

The statistical relationships between winter time temperature/humidity and influenza epidemics in many highly populated regions of northern mid-latitude in the past two decades was also reexamined. However, the identified relations between winter temperature/humidity and influenza epidemics are less robust (see Supplementary Text and Supplementary Figs. S5-S10).

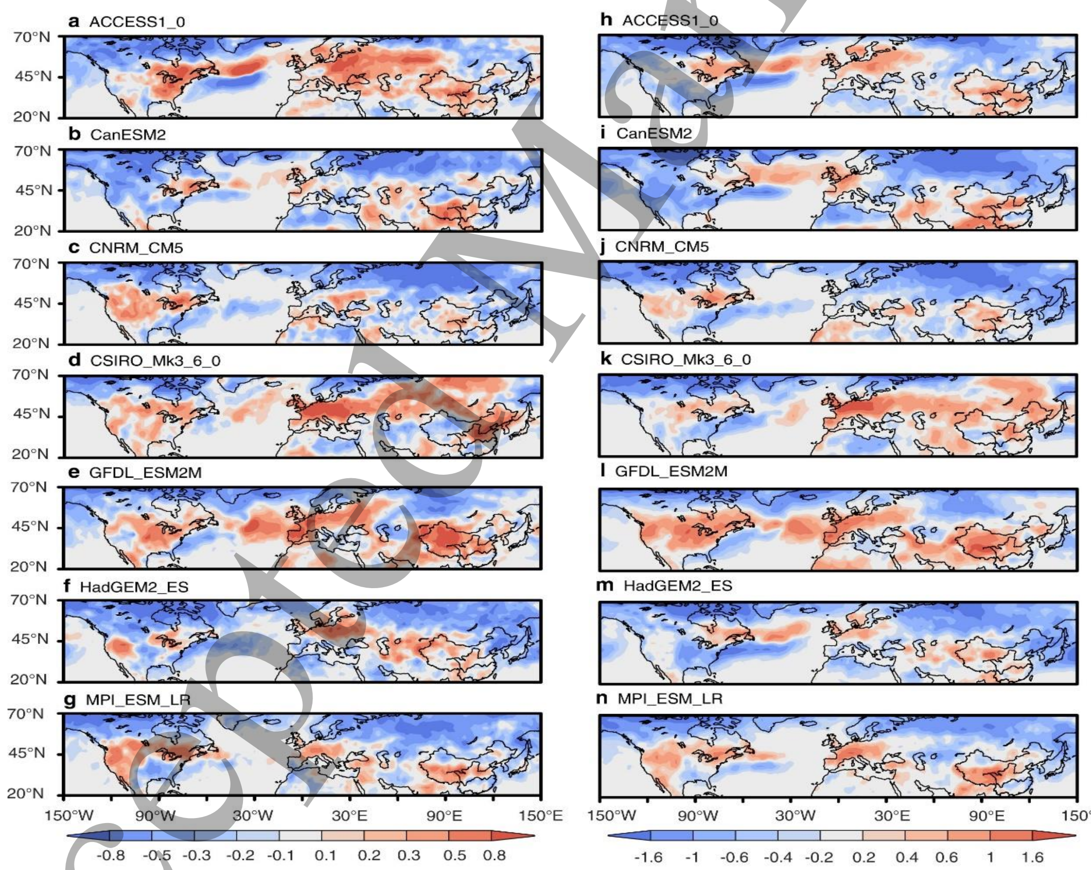

Figure 3. Projected changes in triweekly normalized autumn RWV in a warming climate. a-g, projection of the difference in triweekly normalized autumn RWV of 7 models under RCP8.5 emission scenario during 2020 to 2049 minus that in historical run during 1970 to 1999. h-n, the same to a-g but for 2070 to 2099 replacing the 2020 to 2049.

3.2 Changing risk of influenza in a warming climate

In the past century, the Earth's climate has been changing at an unprecedented pace (Tett *et al* 1999, Wu *et al* 2011), especially in the highly populated northern mid-latitudes. This climate change is not limited only to surface temperature; rather, it also includes changes in other climate variables, such as the mid-latitude synoptic variability (Cohen *et al* 2014, Schneider *et al* 2015). Since the change of RWV can cause the large changes in ILI/IM, as revealed above, understanding the spatial patterns of future RWV can help determining the severity of future ILI/IM threat.

The above identified relation between RWV and ILI/IM provides a chance to estimate the changing risk of influenza epidemic in a warming climate. Figure 3 presents the triweekly RWV changes for two three-decade spans, 2020-2049 and 2070-2099, based on the diagnoses of seven climate system model (Supplementary Table. S1) outputs from Representative Concentration Pathway (RCP) 8.5 emission scenario of the Coupled Model Intercomparison Project Phase 5 (CMIP5) (Taylor *et al* 2012). CMIP5 were used to project future climate in the Intergovernmental Panel on Climate Change's fifth assessment report. The displayed RWV changes are the anomalies of the means of triweekly autumn RWV of the above selected two temporal spans with respect to the historical three-decade mean RWV for the temporal span 1970-1999. While the detailed spatial patterns of RWV changes in these seven models are not exactly same, a common feature emerges: many regions of northern mid-latitudes will have RWV anomaly increase more than 0.5 in the next three decades and more than 1 in the last three decades of the 21st century. Most of these models projected that the highly populated Europe will have the largest RWV increase, with triweekly RWV increase larger than 1 in the next three decades and 2 in the last three decades of the 21st century. This large increase of RWV projects that some regions of the Europe will have the risk of influenza morbidity increase by more than 50% if solely following the statistically robust RWV-IM relation presented in Fig. 1. However, this number may be an overestimation since RWV is not the only cause of the influenza morbidity. All model projected RWV changes in the US show increase only in its highly populated northeast region with a relatively smaller value. The models also projected that the large majority of China will also have RWV increases by up to 1 by the end of the 21st century, implying influenza morbidity will increase by more than 20%. In summary, the increasing RWV is likely to increase the risk of IM in future, although a reliable quantification is out of our reach.

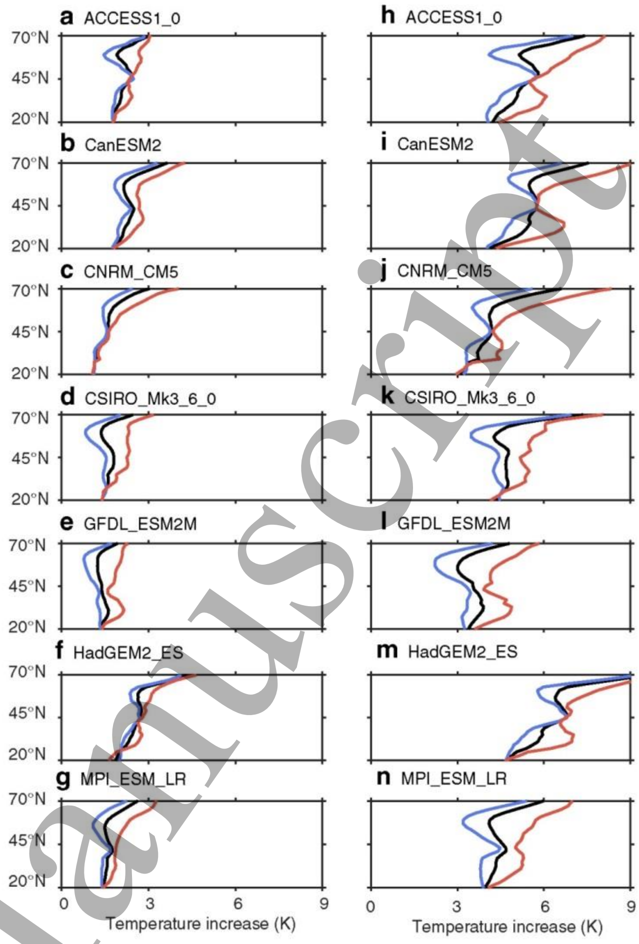

Figure 4. Projected changes in autumn temperature in a warming climate. a-g, projection of the zonal averaged temperature in boreal autumn of 7 models under RCP8.5 emission scenario during 2020 to 2049 minus that in historical run during 1970 to 1999. Unit: K. h-n, the same to a-g but for 2070 to 2099 replacing the 2020 to 2049. The lines in black, blue, and red represent zonal averaged for 130ºW to 120ºE, 130ºW to 30ºE, and 30ºE to 120ºE, respectively.

The validity of above projection of the risk of ILI/IM is highly dependent on the accuracy of the projection of RWV. Is this projected RWV physically justified? The historical data shows that the noticeable land warming after industrial revolution started first in the land neighboring the Arctic and the subtropical northern hemisphere (Ji *et al* 2014). These two bands intensified and generated anomalous temperature gradient that led to the increased anomalous heat transport from polar/subpolar regions and subtropical regions to northern mid-latitude regions in the autumn season. By the end of the 20th century, the maximum warming was at about 50 ºN (Fig. 4), leading to the increased meridional temperature gradient north to that latitude (Ji *et al* 2014). The increased meridional temperature gradient provided a more favorable environment for the synoptic system to develop (Held 1978, Patz *et al* 2005, Altizer 2013), explaining the intensification of RWV. This maximum warming latitude is still shifting southward as the globe continues to warm, see Figure 3 of Ji *et al* (Ji *et al* 2014). The climate projection based on the above mentioned model outputs show that this zone of increased meridional temperature gradient is further south, with its southern edge located at about 45 ºN. Thus, the increased RWV in climate model projection is consistent with previous understandings and can be anticipated. It is noted that, for Asian region, the zone of intensified meridional temperature gradient locates south to the zonally averaged one while for the US and the Europe, that zone locates north to the zonally averaged one.

The similar spatial pattern changes of RWV and zonally averaged temperatures are also seen in the projections under a more moderate emission scenario, RCP4.5. Supplementary Fig. S11 displays the triweekly autumn RWV changes in seven climate system models for a more moderate emission scenario, RCP4.5. The spatial patterns of RWV increase under RCP4.5 resemble these of RCP8.5 (Fig. 3) but with reduced amplitude. Under RCP4.5 emission scenario, many regions of northern mid-latitudes will have RWV anomaly increase more than 0.3 in the next three decades and more than 0.4 in the last three decades of the 21st century. Under the RCP4.5 scenario, the influenza morbidity over Europe and China may increase by more than 30% and 15%, respectively, in the last three decades of the 21st century. In addition, model projections under RCP4.5 emission scenario are characterized by maximum warming over northern mid-latitudes (Supplementary Fig. S12).

4. Discussion

It has been long recognized that the climate change will affect human health and put billions of people at increased risk (Patz *et al* 2005, Altizer *et al* 2013, Costello *et al* 2009). Previous study focused more on the disease dynamics and directly observed temperature and humidity affecting the influenza epidemic. Our study, based on statistical analysis, shows that RWV had also played a significant role in changing the strength of influenza epidemic in the past. In a warming climate, RWV will intensify and the influenza epidemic risk can increase by up to 50% in some northern mid-latitude regions.

It is noted that our identified relation between ILI and RWV is based on the limited data of ILI. The small number of samples may cause bias in the calculation, especially when the data of ILI are highly non-Gaussian. Neverthless, this identified raltion may contribute to earlier preparation and prevention of influenza epidemics. Since an influenza epidemic's peak season is mostly in the second half of winter and autumn RWV contributes significantly to building critical patient levels, the strength of autumn RWV may serve as a valuable predictor of an influenza epidemic in the consequent months.

Finally, it is also noted that the data we analyzed are mostly regional averaged over large spatial domains and age-undistinguished, thereby, the identified statistical relation may contain unknown degree of bias (Lin *et al* 2018, Lin and Chen 2019). In Fig. S4, we presented that the identified RWV-ILI relationship is more robust for preschool children and elderlies. We anticipate that, with fine categorized data potentially available in future, more accurate relationships may be revealed.

Acknowledgements

Q.L. and C.F. are supported by the Chinese Jiangsu Collaborative Innovation Center for Climate Change; Q.L. is also supported by financial support from the program of China Scholarships Council (201706190153); Z.-M.T. is supported by the Natural Science Foundation of China (41461164008); and Z.W. and J.S. are supported by the U.S. National Science Foundation grant (AGS-1723300). The authors declare no competing financial interests.

Data availability statement

The data that support the findings of this study are available from the corresponding author upon reasonable request.

References

[1] Altizer S, Dobson A, Hosseini P, Hudson P, Pascual M and Rohani P 2006 Seasonality and the dynamics of infectious diseases *Ecol. Lett.* **9** 467-484

[2] Altizer S, Ostfeld R S, Johnson P T J, Kutz S and Harvell C D 2013 Climate change and infectious diseases: From evidence to a predictive framework *Science* **341** 514–519

[3] Ballester J, Rodó X, Robine J-M and Herrmann F R 2016 European seasonal mortality and influenza incidence due to winter temperature variability *Nature Clim. Change* **6** 927-931

[4] Baumgartner E A, *et al.* 2012 Seasonality, timing, and climate drivers of influenza activity worldwide *J. Infect. Dis.* **206** 838-846

[5] Bennett J E, Blangiardo M, Fecht D, Elliott P and Ezzati M 2014 Vulnerability to the mortality effects of warm temperature in the districts of England and Wales *Nature Clim. Change* **4** 269-273

[6] Cohen J, *et al.* 2014 Recent Arctic amplification and extreme mid-latitude weather *Nature Geosci.* **7** 627-637

[7] Cohen J 2018 Nasty U.S. flu season continues to intensify *Science* http://dx.doi.org/10.1126/science.aat2020

[8] Costello A, *et al.* 2009 Managing the health effects of climate change *Lancet* **373** 1693-1733

[9] Dalziel B D, Kissler S, Gog J R, Viboud C, Bjørnstad O N, Metcalf C J E and Grenfell B T 2018 Urbanization and humidity shape the intensity of influenza epidemics in U.S. cities *Science* **362** 75-79

[10] Deyle E R, Maher M C, Hernandez R D, Basu S and Sugihara G 2016 Global environmental drivers of influenza *Proc. Natl. Acad. Sci. U.S.A.* **113** 13081-13086

[11] Eurowinter Group 1997 Cold exposure and winter mortality from ischaemic heart disease, cerebrovascular disease, respiratory disease, and all causes in warm and cold regions of Europe *Lancet* **349** 1341–1346

[12] Garten R, *et al.* 2018 Update: Influenza Activity in the United States during the 2017-18 Season and Composition of the 2018-19 Influenza Vaccine *MMWR- Morbid. Mortal. W.* **67** 634-642

[13] Graudenz G S, Landgraf R G, Jancar S, Tribess A, Fonseca S G, Faé K C and Kalil J 2006 The role of allergic rhinitis in nasal responses to sudden temperature changes *J. Allergy Clin. Immun.* **118** 1126-1132

[14] Guo Y, Barnett A G, Yu W, Pan X, Ye X, Huang C and Tong S 2011 A large change in temperature between neighboring days increases the risk of mortality *PLoS One* **6** e16511

[15] Guo Y, *et al.* 2016 Temperature variability and mortality: a multi-country study *Environ. Health. Persp.* **124** 1554-1559

[16] Held I M 1978 The vertical scale of an unstable baroclinic wave and its importance for eddy heat flux parameterizations *J. Atmos. Sci.* **35** 572-576

[17] Ji F, Wu Z, Huang J and Chassignet E P 2014 Evolution of land surface air temperature trend *Nature Clim. Change* **4** 462-466

[18] Kalnay E, *et al.* 1996 The NCEP/NCAR 40-year reanalysis project *Bull. Am. Meteorol. Soc.* **77** 437–471

[19] Li Q, Liu X, Zhang H, Peterson T C and Easterling D T 2004 Detecting and adjusting temporal in-homogeneity in Chinese mean surface air temperature data *Adv. Atmos. Sci.* **21** 260–268

[20] Li Y, Wang X L and Zheng X 2018 Impact of weather factors on influenza hospitalization across different age groups in subtropical Hong Kong *Inter. J. Biometeorol.* **62** 1615-1624

[21] Lin C K, Hsu Y T, Christiani D C, Hung H Y and Lin R T 2018 Risks and burden of lung cancer incidence for residential petrochemical industrial complexes: A meta-analysis and application *Environ. Int*. **121** 404-414

[22] Lin C K and Chen S T 2019 Estimation and application of population attributable fraction in ecological studies *Environ. Health* **18** 52

[23] Loh E, Kugelberg E, Tracy A, Zhang Q, Gollan B, Ewles H, Chalmers R, Pelicic V and Tang C M 2013 Temperature triggers immune evasion by Neisseria meningitidis *Nature* **502** 237-240

[24] Lowen A C, Mubareka S, Steel J and Palese P 2007 Influenza virus transmission is dependent on relative humidity and temperature *PLoS Pathog.* **3** e151

[25] Lowen A C and Steel J 2014 Roles of humidity and temperature in shaping influenza seasonality *J. Virol.* **88** 7692-7695

[26] Mirsaeidi M, Motahari H, Khamesi M T, Sharifi A, Campos M A and Schraufnagel D E 2016 Climate change and respiratory infections *Ann. Am. Thorac. Soc.* **13** 1223-1230

[27] Munster V J, *et al.* 2009 Pathogenesis and transmission of swine-origin 2009 A(H1N1) influenza virus in ferrets *Science* **325** 481-483

[28] Patz J A, Campbell-Lendrum D, Holloway T and Foley J A 2005 Impact of regional climate change on human health *Nature* **438** 310–317

[29] Petrova V N and Russell C A 2018 The evolution of seasonal influenza viruses *Nature Rev. Microbiol.* **16** 47-60

[30] Polozov I V, Bezrukov L, Gawrisch K and Zimmerberg J 2008 Progressive ordering with decreasing temperature of the phospholipids of influenza virus *Nature Chem. Biol.* **4** 248-255

[31] Schneider T, Bischoff T and Plotka H 2015 Physics of changes in synoptic midlatitude temperature variability *J. Climate* **28** 2312-2331

[32] Shaman J and Kohn M 2009 Absolute humidity modulates influenza survival, transmission, and seasonality *Proc. Natl. Acad. Sci. U.S.A.* **106** 3243-3248

[33] Shaman J, Pitzer V E, Viboud C, Grenfell B T, Lipsitch M 2010 Absolute humidity and the seasonal onset of influenza in the continental United States. *PLoS Biol.* **8** e1000316

[34] Smith G J D, *et al.* 2009 Origins and evolutionary genomics of the 2009 swine-origin H1N1 influenza A epidemic *Nature* **459** 1122-1125

[35] Staddon P L, Montgomery H E and Depledge M H 2014 Climate warming will not decrease winter mortality *Nature Clim. Change* **4** 190-194

[36] Taylor K E, Stouffer R J and Meehl G A 2012 An overview of CMIP5 and the experiment design *Bull. Am. Meteorol. Soc.* **4** 485–498

[37] Tett S F B, Stott P A, Allen M R, Ingram M J and Mitchell J F B 1999 Causes of twentieth-century temperature change near the Earth's surface *Nature* **399** 569-572

[38] Togias A G, Naclerio R M, Proud D, Fish J E, Adkinson N F, Kagey-Sobotka Jr A, Norman P S and Lichtenstein L M 1985 Nasal challenge with cold, dry air results in release of inflammatory mediators. Possible mast cell involvement *J. Clin. Investig.* **76** 1375–1381

[39] Viboud C, Bjørnstad O N, Smith D L, Simonsen L, Miller M A and Grenfell B T 2006 Synchrony, waves, and spatial hierarchies in the spread of influenza *Science* **312** 447-451

[40] Vijaykrishna D, *et al.* 2011 Long-term evolution and transmission dynamics of swine influenza a virus *Nature* **473** 519-522

[41] Walther B A and Ewald P W 2004 Pathogen survival in the external environment and the evolution of virulence *Biol. Rev.* **79** 849-869

[42] Wei Y, *et al*. 2019 Associations between seasonal temperature and dementia-associated hospitalizations in New England *Environment International* **126** 228-233

[43] Wu F, Fu C, Qian Y, Gao Y and Wang S 2017 High-frequency daily temperature variability in China and its relationship to large-scale circulation *Int. J. Climatol.* **37** 570-582

[44] Wu Z, Huang N E, Wallace J M, Smoliak B V and Chen X 2011 On the time-varying trend in global-mean surface temperature *Clim. Dynam.* **37** 759-773

[45] Yang W, Lipsitch M and Shaman J 2015 Inference of seasonal and pandemic influenza transmission dynamics *Proc. Natl. Acad. Sci. U.S.A.* **112** 2723-2728

[46] Zhan Z, Zhao Y, Pang S, Zhong X, Wu C and Ding Z 2017 Temperature change between neighboring days and mortality in United States: a nationwide study *Sci. Total Environ.* **584** 1152-1161

Figure Caption List

Figure 1. Long-term ILI/IM changes with respect to RWV. a, Weekly lagged correlation between triweekly RWV anomaly and ILI/IM anomaly for period 1997-2018 over the whole USA. b-d, the same as a but for the mainland China (2005-2018), Italy (2000-2018), and France (1997-2015), respectively. e, the scattered plot of the pairs of peak ILI/IM and the averaged triweekly RWV over the temporal span marked by red interval immediately above each left panels, for the USA over the temporal span of 1997-2018, with the stars correspond to 2017-2018 influenza season. f-h, the same as e, but for mainland China (2005-2018), Italy (2000-2018), and France (1997-2015), respectively.

Figure 2. The spatial patterns of ILI/IM and RWV during 2017-2018 influenza season. a, U.S. ILI/IM anomaly (%) averaged over January-February 2018; b-c, Monthly averaged RWV anomaly (days) over U.S. from October 15-November 15, 2017 and January-February 2018, respectively; d, the same as a but for Europe. e-f, Monthly averaged RWV anomaly (days) over Europe from September 2017 and January-February 2018, respectively; Black represents missing records.

Figure 3. Projected changes in triweekly normalized autumn RWV in a warming climate. a-g, projection of the difference in triweekly normalized autumn RWV of 7 models under RCP8.5 emission scenario during 2020 to 2049 minus that in historical run during 1970 to 1999. h-n, the same to a-g but for 2070 to 2099 replacing the 2020 to 2049.

Figure 4. Projected changes in autumn temperature in a warming climate. a-g, projection of the zonal averaged temperature in boreal autumn of 7 models under RCP8.5 emission scenario during 2020 to 2049 minus that in historical run during 1970 to 1999. Unit: K. h-n, the same to a-g but for 2070 to 2099 replacing the 2020 to 2049. The lines in black, blue, and red represent zonal averaged for 130ºW to 120ºE, 130ºW to 30ºE, and 30ºE to 120ºE, respectively.